Available online at www.sciencedirect.com

SCIENCE DIRECT

European Journal of Pharmacology 516 (2005) 139 – 144

www.elsevier.com/locate/ejphar

Autoradiographic localisation of [^{3}H]2-BFI imidazoline I_2 binding sites in mouse brain

Nicholas MacInnes*, Sheila L. Handley

Pharmaceutical Sciences Research Institute, Aston University, Birmingham, B4 7ET, United Kingdom

Received 2 March 2005; received in revised form 23 March 2005; accepted 8 April 2005
Available online 31 May 2005

Abstract

Imidazoline I_2 binding sites are heterogeneous in nature and have been observed in the brain of a number of species. Development of specific imidazoline I_2 radioligands, such as [^{3}H]2-BFI and [^{3}H]BU224, that have a high affinity for the imidazoline I_2 binding site, has enabled the central distribution of these sites to be mapped. Extensive studies have been conducted on the rat brain with a number of radioligands. However, to date a comprehensive analysis of imidazoline I_2 ligand binding in mouse brain has not been completed. In the present work we describe levels of [^{3}H]2-BFI specific binding found throughout the mouse brain.

[^{3}H]2-BFI (2 nM) showed discrete regional distribution which was readily displaced by saturating concentrations of the specific imidazoline I_2 ligand BU224. The highest levels of [^{3}H]2-BFI specific binding were found in the dorsal raphe, paraventricular thalamus and nucleus accumbens. Moderate levels were found throughout the lining of the aqueduct, lateral ventricle, lateral 4th ventricle, 4th ventricle, 3rd ventricle, but not the dorsal 3rd ventricle.

Based on the loss of [^{3}H]idazoxan binding in brain homogenates from monoamine oxidase-A and B (MAO-A and MAO-B) deficient mice it has been suggested that imidazoline I_2 binding sites are predominantly on MAO. Consistent with this hypothesis the regional distribution of [^{3}H]2-BFI shows some overlap with that previously reported for MAO. However, in the rat imidazoline I_2 binding sites have been shown to be heterogeneous in nature and it is likely [^{3}H]2-BFI is binding to multiple imidazoline I_2 binding sites within mouse brain.

Keywords: Imidazoline I_2 binding site; [^{3}H]2-BFI; Autoradiography; MAO-B; Brain; (Mouse)

1. Introduction

Imidazoline binding sites have been separated into three classes, imidazoline$_1$, imidazoline$_2$ and imidazoline$_3$, based on their affinity for the imidazolines clonidine, idazoxan and ethoxy-idazoxan (Eglen et al., 1998). The specific imidazoline I_2 ligand 2-BFI (2-(-2-benzofuranyl)-2-imidazoline) and its quinoline and isoquinoline analogues BU 216, 224 and 226 show a high affinity in vitro for the imidazoline I_2 binding site (Lione et al., 1998). Drug discrimination studies have indicated functional consequences of imidazoline I_2 ligand binding in vivo (MacInnes and Handley, 2003) and imidazoline I_2 ligands have been shown to increase food intake (Polidori et al., 2000), decrease immobility in the forced-swim test (Finn et al., 2003), potentiate morphine analgesia (Sánchez-Blázquez et al., 2000) and increase plasma corticosterone levels (Finn et al., 2004). A range of imidazoline binding proteins, with molecular weights between 27 and 85 kDa have been visualised or purified from a number of species and tissues (Escriba et al., 1999) but their functional significance is unknown as a second-messenger system has not been established for the imidazoline I_2 binding site. However, one of these proteins may be creatine kinase (Kimura et al., 2003) and a further two represent the A and the B forms of monoamine oxidase (Remaury et al., 2000). In vitro several imidazoline I_2 ligands, including 2-BFI and BU224, reversibly inhibit MAO (Lalies et al., 1999), whilst in vivo MAO inhibitors substitute for 2-

* Corresponding author. Present address: Wolfson Centre for Age Related Disease, Guys Kings and St Thomas' School of Biomedical Sciences, Kings College, London, SE1 1UL, United Kingdom. Tel.: +44 207 848 6680; fax: +44 207 848 6145.
E-mail address: nicholas.macinnes@kcl.ac.uk (N. MacInnes).

0014-2999/$ - see front matter © 2005 Elsevier B.V. All rights reserved.
doi:10.1016/j.ejphar.2005.04.006

BFI in a two lever drug discrimination paradigm (MacInnes and Handley, 2002), and 2-BFI potentiates L-3,4-dihydroxyphenylamine (L-DOPA) induced circling in the 6-hydroxydopamine model of Parkinson's Disease (MacInnes and Duty, 2004). Additionally, studies conducted in transgenic MAO-A and MAO-B knockout mice, indicate brain [^{3}H]idazoxan-labelled imidazoline I_2 binding sites are predominantly, although not exclusively (Kimura et al., 2003), associated with MAO (Remaury et al., 2000).

Autoradiographic studies of central imidazoline I_2 binding sites, as defined by [^{3}H]idazoxan or the specific imidazoline I_2 ligands [^{3}H]-RS-45041-190 ([^{3}H]4-chloro-2-(imidazolin-2-yl) isoindoline), [^{3}H]2-BFI and [^{3}H]BU224 have indicated these sites can be found within a variety of species, e.g., rabbit (Lione et al., 1997), rat (MacKinnon et al., 1995; Lione et al., 1998; MacInnes and Handley, 2001; Robinson et al., 2002) chicken (Danbury et al., 1999), frog (Tyacke et al., 1999) and human (De Vos et al., 1994). In rat these radioligands consistently label the dorsal raphe, interpeduncular nucleus and circumventricular organs (arcuate nucleus, area postrema, ependyma and pineal gland; MacKinnon et al., 1995; Lione et al., 1998; Robinson et al., 2002; MacInnes and Handley, 2004).

Despite the widespread use of naïve and transgenic mice in studies on imidazoline I_2 binding sites, the autoradiographic distribution of these sites has not been previously assessed. Hence, using quantative receptor autoradiography, the aim of the current study was to examine the distribution of central imidazoline I_2 binding sites in naïve mouse brain.

2. Method

2.1. Animals and drug treatment

Six male, 5-week-old, drug naive C/57B mice (housed under a controlled light/dark cycle; 25–30 g) were anaesthetised with fluothane, decapitated and their brains rapidly frozen with crushed dry ice. Tissues were stored at −70 until sectioning began.

2.2. Autoradiography

Transverse sections (12 μM) were cut at −16 °C on a cryostat (Bright OTF, Bright Instruments, UK) and thaw mounted onto Chrom-alum gelatin coated slides. Mounted sections were stored at −70 °C until used. Nuclei of interest were identified by comparison with adjacent 30 μM cresyl violet stained sections according the mouse brain atlas of Franklin and Paxinos (1997).

Sections were thawed for 45 min and pre-washed for 30 min at room temperature (21–25 °C) in 50 mM Tris HCl buffer (pH 7.4) containing 1 mM $MgCl_2$ (magnesium chloride); laid out on tissue paper and dried under a stream of cool air. Sections were then incubated for 40 min in 100 μl assay buffer containing 2 nM [^{3}H]2-BFI for total binding (preliminary data indicated 2 nM was optimal for reducing non-specific binding levels to background), 10 μM BU224 was used to determine non-specific binding. Incubation was stopped by aspiration of buffer; sections were then washed twice for 10 s in ice cold buffer, dipped once in ice cold distilled water; dried rapidly under a stream of cool air; mounted in autoradiography cases (Genetic Research Instrumentation, Braintree, UK) together with activated [^{3}H]-microscale standards (Amersham, UK) and apposed to [^{3}H]-Hyperfilm (Amersham, UK) for 6 weeks.

Autoradiography films were developed for 90 s in Ilford High Contrast developer (1 part developer to 9 parts distilled water), immersed in acetic acid (0.01%) for 20 s and fixed with Ilford Hypam fixer (1 part fixer to 4 parts distilled water) plus Ilford rapid hardener (1 part hardener to 50 parts distilled water) for 6 min; washed in distilled water containing wetting agent (1 part wetting agent to 200 parts distilled water) for 20 min to prevent spotting and air dried. Autoradiograms were quantified by computer-assisted densitometry (MCID version 4, Microcomputer Image Device, Imaging Research, St Catherines, OT, Canada) and values were converted to fmol [^{3}H]2-BFI/mg wet tissue using [^{3}H]-microscale standards. For each nucleus examined, one datum point was obtained for each rat. These data points were the mean obtained by collapsing the results from 3 sections per nucleus and three determinations per section. Data were derived from five or six mice.

2.3. Drugs

BU224 (2-[4,5-dihydroimidaz-2-yl]-quinoline hydrochloride) was purchased from Tocris (UK). [^{3}H]2-BFI ([5,7-(*n*)-^{3}H]2-(2-Benzofuranyl)-2-imidazoline; specific activity 70 Ci/mmol; radioactive concentration 200 μCi/ml) was purchased from Amersham (UK) and all other reagents were purchased from Sigma (UK).

3. Results

The distribution of [^{3}H]2-BFI labelled imidazoline I_2 binding sites showed discrete regionalisation within the mouse brain (Fig. 1). Non specific binding, defined by the quantity of [^{3}H]2-BFI bound to an adjacent section under saturating concentrations of BU224, was low (<10%; Fig. 1B). Comparison of autoradiograms to radioactive standards gave rise to the fmol/mg tissue levels of specific binding reported in Table 1.

All areas of the cortex, cerebellum hippocampus and olfactory bulb showed low levels (<25 fmol/mg tissue) of [^{3}H]2-BFI specific binding (Table 1) with the lowest level in the olfactory bulb granular layer (5.63 fmol/mg tissue). With the exception of the nucleus accumbens (59.20 fmol/mg tissue; Fig. 1C) low levels of specific binding were seen throughout the basal ganglia. High levels of specific binding were evident in the paraventricular thalamus (>50 fmol/mg tissue; Fig. 1D) and moderate levels within the reunions thalamic group.

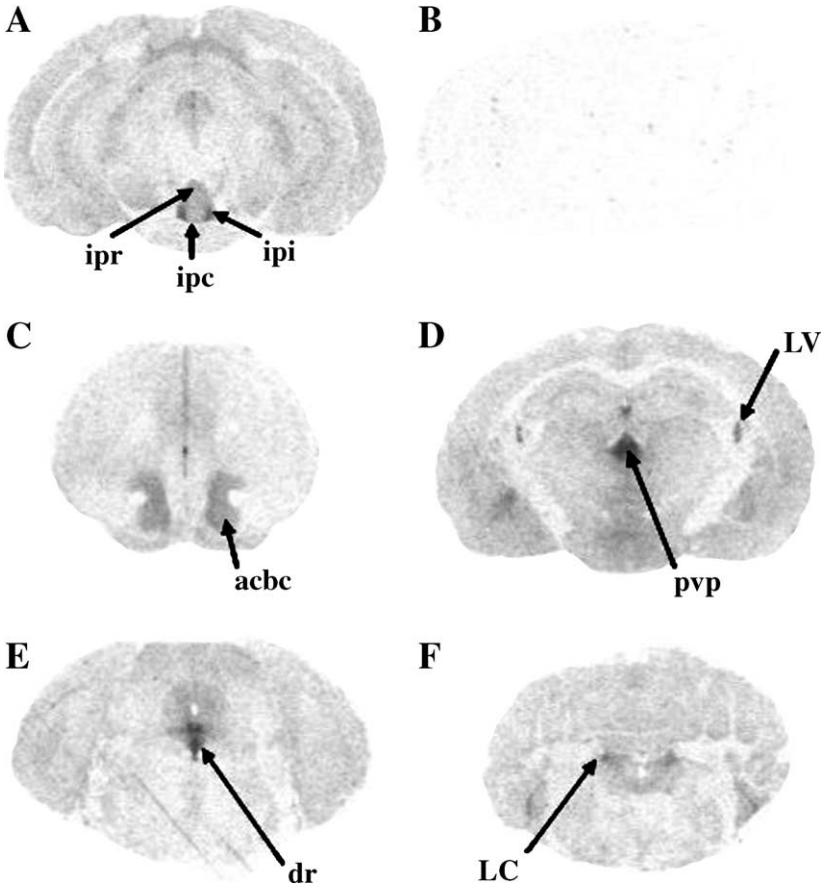

Fig. 1. Autoradiograms showing specific binding (A, C, D, E, F) and non-specific binding (B) of 2 nM [^{3}H]2-BFI to transverse mouse brain sections. Sections are shown in a rostral–caudal direction taken at, (A and B) −3.80 mm posterior to bregma, (C) 1.34 mm anterior to bregma and (D) −2.18 mm, (E), −4.48 mm (F), −5.80 mm posterior to bregma. See Table 1 for key to abbreviations.

Similarly, most areas of the hypothalamus except for the ventral tuberomammillary nucleus (44.59 fmol/mg tissue) showed low levels of [^{3}H]2-BFI specific binding. The interpeduncular nuclei (Ip) showed moderate to high levels of specific binding and [^{3}H]2-BFI appeared to selectively label individual subnuclei within this region (Fig. 1A and Table 1). The rostral and caudal interpeduncular subnuclei only exhibited moderate levels of specific binding (27.45 and 24.13 fmol/mg tissue respectively) whilst the lateral/intermediate subnuclei had much higher levels levels (51.74 fmol/mg tissue). The highest levels of [^{3}H]2-BFI specific binding were found within the dorsal raphe (dr; 76.04 fmol/mg tissue; Fig. 1E) and moderate levels within the locus coeruleus (49.81 fmol/mg tissue; Fig. 1F).

With the exception of the 3rd ventricle, levels of specific binding within the lining of the ventricular system were either moderate of high. In contrast all circumventricular organs assessed, with the exception of the area postrema (43.57 fmol/mg tissue), showed low levels of specific binding.

4. Discussion

[^{3}H]2-BFI imidazoline I_2 binding sites exhibit a discrete regional distribution in rat brain (Lione et al., 1998; MacInnes and Handley, 2001). A similar pattern of binding was seen here in mouse brain with [^{3}H]2-BFI labelling many of the same nuclei with high intensity, i.e., the lining of the ventricles, paraventricular, interpenduncular nucleus, dorsal raphe and areas of the paraventricular thalamus. However, there were a number of notable discrepancies. In the rat [^{3}H]2-BFI and [^{3}H]-RS-45041-190 show the highest levels of specific binding within the arcuate nucleus (Lione et al., 1998; MacInnes and Handley, 2001) and subfornical organ (MacKinnon et al., 1995) while these areas were only weakly labelled in the mouse. In the mouse the dorsal raphe showed the highest intensity of ligand binding followed by the posterior paraventricular thalamus (pvp), although the pvp and dorsal raphe exhibited only moderate binding in the rat (Lione et al., 1998; MacKinnon et al., 1995). It remains to be established if these differences represent species specific differences in creatine kinase, MAO, or another, as yet unidentified, imidazoline I_2 binding site.

The distribution of creatine kinase has not been mapped in either rat or mouse brain, but MAO-B distribution has (Saura et al., 1992) and its distribution compares favourably with the present data. In mouse,

Table 1
Distribution of [^{3}H]2-BFI specific binding in mouse brain sections

Specific binding [^{3}H]2-BFI (fmol/mg tissue)			
Brain region	Abb.	Mean	S.E.M.
Cortical areas			
Visual cortex	V	12.18	0.74
Motor cortex	M	11.09	1.07
Sensory cortex	S	10.19	0.83
Auditory cortex	A	10.00	1.53
Cingulate cortex	Cg	16.57	1.68
Piriform cortex	pir	9.40	0.96
Entorhinal cortex	Ent	14.63	0.90
Olfactory bulb			
Granule layer olfactory bulb	gro	5.63	0.95
Mitral cell layer	mit	16.28	2.38
Olfactory tubercle	tu	24.54	2.01
Cerebellum			
White matter	1	4.77	0.48
Dense granules	2	9.71	0.80
Purkinje cells	3	21.19	1.13
Molecular layer	4	7.62	0.58
Hippocampus			
CA1 field of the hippocampus	CA1	9.30	1.31
CA2 field of the hippocampus	CA2	7.90	0.96
CA3 field of the hippocampus	CA3	9.05	1.09
Dentate gyrus	dg	11.90	1.38
Hippocampal fissure	Hif	16.44	1.00
Subiculum	s	12.86	1.92
Basal ganglia			
Lateral globus pallidus	lgp	12.03	1.02
Caudate putamen	cpu	18.83	1.78
Accumbens nucleus	acbc	59.20	4.26
Hypothalamus			
Ventromedial	vm	16.25	1.75
Dorsomedial	dm	21.71	2.45
Medial mammillary nuc.	ml	18.05	2.16
Ventral tuberomammillary nucleus	vtm	44.59	6.90
Superior colliculus	su	14.95	1.44
Superior colliculus superficial gray	sug	28.51	2.27
Thalamus			
Paraventricular thalamus			
Posterior	pvp	72.19	8.81
Medial	pv	70.52	8.13
Anterior	pva	63.16	8.25
Geniculate nucleus	mg	15.05	1.76
Posterior thalamic nucleus	lp	15.79	1.92
Mediodorsal thalamic nucleus	md	18.64	2.20
Posterior thalamic nuclear group	po	10.72	1.31
Reuniens thalamic group	re	42.41	4.51
Substantia nigra	snr	19.62	1.22
Midbrain			
Interpeduncular nucleus			
Rostral subnuclei	ipr	27.45	2.34
Caudal subnuclei	ipc	24.13	1.48
Lateral/intermediate subnuclei	ipi/lpi	51.74	4.11
Pons			
Solitary tract	sol	27.47	2.12
Inferior olives	io	23.31	1.07
Peri-aqueductal gray	pag	23.11	0.69
Locus coeruleus	LC	49.81	3.07
Dorsal raphe	dr	76.04	2.30
Circumventricular organs			
Area postrema	Ap	43.57	2.97
Arcuate nucleus	Arc	17.50	2.95
Median eminence	me	14.73	1.79
Subfornical organ	SFO	16.86	2.44
Ventricles			
Aqueduct	Aq	65.33	6.58
3rd ventricle	3V	21.80	3.17
Dorsal 3rd ventricle	D3V	57.31	4.50
Lateral ventricle	LV	54.14	6.81
Lateral 4th ventricle	L4V	65.73	4.51
4th ventricle	4V	47.66	5.00

Results are shown as mean and S.E.M (standard error of the mean; fmol/mg wet tissue equivalent). Mean readings were derived by collapsing the results from 3 sections per nucleus and three determinations per section. Data was derived from five or six mice. Abbreviations, 3rd ventricle, 3V; 4th ventricle, 4V; accumbens nucleus, acbc; anterior paraventricular thalamus, pva; aqueduct, Aq; arcuate nucleus, Arc; area postrema, Ap; auditory cortex, A; CA1 field of the hippocampus, CA1; CA2 field of the hippocampus, CA2; CA3 field of the hippocampus, CA3; caudal interpeduncular subnuclei, ipc; caudate putamen, cpu; cingulate cortex, Cg; dense granules, 2; dentate gyrus, dg; dorsal 3rd ventricle, D3V; dorsal raphe, dr; dorsomedial, dm; entorhinal cortex, Ent; geniculate nucleus, mg; granule layer olfactory bulb, gro; hippocampal fissure, Hif; inferior olives, io; lateral 4th ventricle, L4V; lateral globus pallidus, lgp; lateral ventricle, LV; lateral/intermediate interpeduncular subnuclei, ipi/lpi; locus coeruleus, LC; medial mammillary nucleus, ml; medial paraventricular thalamus, pv; median eminence, me; mediodorsal thalamic nucleus, md; mitral cell layer, mit; molecular layer, 4; motor cortex, M; olfactory tubercle, tu; peri-aqueductal gray, pag; piriform cortex, pir; posterior paraventricular thalamus, pvp; posterior thalamic nuclear group, po; posterior thalamic nucleus, lp; purkinje cells, 3; reuniens thalamic group, re; rostral interpeduncular subnuclei, ipr; sensory cortex, S; solitary tract, sol; subfornical organ, SFO; subiculum, s; substantia nigra, snr; superior colliculus superficial gray, sug; superior colliculus, su; ventral tuber-omammillary nucleus, vtm; ventromedial, vm; visual cortex, V; white matter, 1.

the reversible MAO-B inhibitor [^{3}H]Ro19-6327 (Lazabemide) showed high levels of specific binding in the, dorsal raphe, ependyma of the ventricles, paraventricular thalamic nuclei and nucleus accumbens (Saura et al., 1994), which is similar to the binding profile of [^{3}H]2-BFI shown here. However, [^{3}H]2-BFI labelled these regions with considerably less of the ligand (fmol/mg protein range) than was the case with [^{3}H]Ro19-6327 (nmol/mg protein range). Both studies use a concentration of the tritiated ligand close to the K_D and it is therefore unlikely these differences in specific binding can be accounted for solely by the ligand concentration used. Indeed homogenate radioligand binding studies conducted in the rat have shown [^{3}H]2-BFI (B_{max}, 144 fmol/mg; Lione et al., 1998) binds to considerably fewer sites than [^{3}H]Ro19-6327 (B_{max}, 3.45 pmol/mg; Saura et al., 1992). It is presently unclear what accounts for these differences.

One of the notable features in the present data are the levels of specific binding evident within the ependyma or ventricular lining. The ependymal surface is primarily made up of tannocytes (Bruni, 1998) which contain high levels of MAO-B (Saura et al., 1994; Bruni, 1998) and,

during fetal life, GFAP (Glial fibrillary acidic protein; Sarnat, 1998). The imidazoline I_2 specific ligand LSL60101, has been shown to increase both GFAP protein and [^{3}H]idazoxan imidazoline I_2 binding in the rat brain, although its cogener, the imidazoline I_2 ligand LSL60125 does not (Olmos et al., 1994; Alemany et al., 1995). However, as ependymal tannocyte GFAP expression does not continue into adult hood (Sarnat, 1998) and in a rodent model of global forebrain ischaemia, hippocampal astrocytic GFAP mRNA expression, but not [^{3}H]2-BFI binding, was shown to increase in response to vascular injury (Conway et al., 1998) it appears unlikely that ependymal binding of [^{3}H]2-BFI is to GFAP.

In conclusion, the present data reports the discrete regional distribution of [^{3}H]2-BFI in mouse brain. This distribution showed broad agreement with the distribution of this binding in rat brain and similarities were observed with the distribution of MAO-B inhibitor [^{3}H]19-6327 binding previously seen in mouse brain.

Acknowledgements

We would like to thank Dr. J.G. Richards (Hoffmann-La Roche, Basel, Switzerland) for his extensive help with autoradiography. We would also like to thank the BBSRC who supported this work.

References

Alemany, R., Olmos, G., Escriba, P.V., Menargues, A., Obach, R., Garcia-Sevilla, J.A., 1995. LSL 60101, a selective ligand for imidazoline I_2 receptors, on glial fibrillary acidic protein concentration. Eur. J. Pharmacol. 280, 205–210.

Bruni, J.E., 1998. Ependymal development, proliferation, and functions: a review. Microsc. Res. Tech. 41, 2–15.

Conway, E.L., Gundlach, A.L., Craven, J.A., 1998. Temporal changes in glial fibrillary acidic protein messenger RNA and [^{3}H]PK11195 binding in relation to imidazoline I_2-receptor and alpha(2)-adrenoceptor binding in the hippocampus following transient global forebrain ischaemia in the rat. Neuroscience 82, 805–817.

Danbury, T.C., Ruban, B., Hudson, A.L., Waterman-Pearson, A.E., Kestin, S.C., 1999. Imidazoline (I_2) binding sites in chicken brain. Ann. N.Y. Acad. Sci. 881, 189–192.

De Vos, H., Bricca, G., De Keyser, J., De Backer, J.P., Bousquet, P., Vauquelin, G., 1994. Imidazoline receptors, non-adrenergic idazoxan binding sites and α_2-adrenoceptors in the human central nervous system. Neuroscience 50, 589–598.

Eglen, R.M., Hudson, A.L., Kendall, D.A., Nutt, D.J., Morgan, N.G., Wilson, V.G., Dillon, M.P., 1998. 'Seeing through a glass darkly': casting a light on imidazoline 'I' sites. Trends Pharmacol. Sci. 19, 381–390.

Escriba, P.V., Ozaita, A., Garcia-Sevilla, J.A., 1999. Pharmacologic characterisation of imidazoline receptor proteins identified by immunologic techniques and other methods. Ann. N.Y. Acad. Sci. 881, 8–25.

Finn, D.P., Marti, O., Harbuz, M.S., Valles, A., Belda, X., Marquez, C., Jessop, D.S., Lalies, M.D., Armario, A., Nutt, D.J., Hudson, A.L., 2003. Behavioural, neuroendocrine and neurochemical effects of the imidazoline I_2 receptor selective ligand BU224 in naive rats and rats exposed to the stress of the forced swim test. Psychopharmacology 167, 195–202.

Finn, D.P., Hudson, A.L., Kinoshita, H., Coventry, T.L., Jessop, D.S., Nutt, D.J., Harbuz, M.S., 2004. Imidazoline I_2 receptor- and α_2-adrenoceptor-mediated modulation of hypothalamic–pituitary–adrenal axis activity in control and acute restraint stressed rats. J. Psychopharmacol. 18, 43–50.

Franklin, K.B.J., Paxinos, G., 1997. The Mouse Brain in Stereotaxic Coordinates. Academic Press, UK.

Kimura, A., Tyacke, R.J., Minchin, M.C., Nutt, D.J., Hudson, A.L., 2003. Identification of an I_2 binding protein from rabbit brain. Ann. N.Y. Acad. Sci. 1009, 364–366.

Lalies, M.D., Hibell, A., Hudson, A.L., Nutt, D.J., 1999. Inhibition of central monoamine oxidase by imidazoline$_2$ site selective ligands. Ann. N.Y. Acad. Sci. 881, 114–117.

Lione, L.A., Nutt, D.J., Hudson, A.L., 1997. Autoradiographical localisation of imidazoline I-2 sites labelled with [^{3}H]-2-(-2-Benzofuranyl)-2-imidazoline in rabbit brain. Br. J. Pharmacol. 122, 65.

Lione, L.A., Nutt, D.J., Hudson, A.L., 1998. Characterisation and localisation of [^{3}H]2-(2-benzofuranyl)-2-imidazoline binding in the rat brain: a selective ligand for imidazoline I_2 receptors. Eur. J. Pharmacol. 353, 123–135.

MacInnes, N., Duty, S., 2004. Locomotor effects of imidazoline-I_2 site specific ligands and monoamine oxidase inhibitors in rats with a unilateral 6-hydroxydopamine lesion of the nigrostriatal pathway. Br. J. Pharmacol. 143, 952–959.

MacInnes, N., Handley, S.L., 2001. Region-dependent effects of acute and chronic tranylcypromine in vivo on [^{3}H]2-BFI binding to brain imidazoline I_2 sites. Eur. J. Pharmacol. 428, 221–225.

MacInnes, N., Handley, S.L., 2002. Characterisation of the discriminable stimulus produced by 2-BFI: effects of imidazoline I_2-site ligands, MAOIs, β-carbolines, agmatine and ibogaine. Br. J. Pharmacol. 135, 1227–1234.

MacInnes, N., Handley, S.L., 2003. Potential serotonergic and noradrenergic involvement in the discriminative stimulus effects of the selective imidazoline I_2-site ligand 2-BFI. Pharmacol. Biochem. Behav. 75, 427–433.

MacInnes, N., Handley, S.L., 2004. Chronic administration of 2-(-2-benzofuranyl)-2-imidazoline (2-BFI) induces region specific increases in [^{3}H]2-BFI imidazoline-I_2-site binding in the brain. Neurochem. Lett. 363, 11–13.

MacKinnon, A.C., Redfern, W.S., Brown, C.M., 1995. [^{3}H]-RS-45041-190: a selective high affinity radioligand for I_2 imidazoline receptors. Br. J. Pharmacol. 116, 1729–1736.

Olmos, G., Almenay, R., Escriba, P.V., Garcia-Sevilla, J.A., 1994. The effects of chronic imidazoline drug treatment on glial acidic protein concentrations in rat brain. Br. J. Pharmacol. 111, 997–1002.

Polidori, C., Gentili, F., Pigini, M., Quaglia, W., Panocka, I., Massi, M., 2000. Hyperphagic effect of novel compounds with high affinity for imidazoline I_2 binding sites. Eur. J. Pharmacol. 392, 41–49.

Remaury, A., Raddatz, R., Ordener, C., Savic, S., Shih, J.C., Che, K., Seif, I., De Maeyer, E., Lanier, S.M., Parini, A., 2000. Analysis of the pharmacological and molecular heterogeneity of I_2-imidazoline-binding proteins using monoamine oxidase-deficient mouse models. Mol. Pharmacol. 58, 1085–1090.

Robinson, E.S., Tyacke, R.J., Nutt, D.J., Hudson, A.L., 2002. Distribution of [^{3}H]BU224, a selective imidazoline I_2 binding site ligand, in rat brain. Eur. J. Pharmacol. 450, 55–60.

Sánchez-Blázquez, P., Assumpico Boronat, M., Olmos, G., Garcia-Sevilla, J.A., Garzon, J., 2000. Activation of I_2-imidazoline receptors enhances supraspinal morphine analgesia in mice: a model to detect agonist and antagonist activities at these receptors. Br. J. Pharmacol. 130, 146–152.

Sarnat, H.B., 1998. Histochemistry and immunocytochemistry of the developing ependyma and choroid plexus. Microsc. Res. Tech. 41, 14–28.

Saura, J., Kettler, R., Da Prada, M., Richards, J.G., 1992. Quantitive enzyme radioautography with [^{3}H]Ro-41-1049 and [^{3}H]Ro-19-6327 in vitro: localisation and abundance of MAO-A and MAO-B in rat CNS, peripheral organs and human brains. J. Neurosci. 12, 1977–1999.

Saura, J., Richards, J.G., Mahy, N., 1994. Differential age-related changes of MAO-A and MAO-B in mouse brain and peripheral organs. Neurobiol. Aging 15, 399–408.

Tyacke, R.J., Nutt, D.J., Hudson, A.L., 1999. Autoradiography of I_2 receptors in frog brain. Ann. N.Y. Acad. Sci. 881, 208–211.